Acquisition of resistance to wild-type spike-immune sera by emerging SARS-CoV-2 variants

Hisashi Arase (arase@biken.osaka-u.ac.jp)
Osaka University https://orcid.org/0000-0002-1153-3166

Yafei Liu
Osaka University

Noriko Arase
Graduate School of Medicine, Osaka University https://orcid.org/0000-0003-3966-3437

Jun-ichi Kishikawa
Institute for Protein Research, Osaka University

Mika Hirose
Osaka University https://orcid.org/0000-0001-8991-587X

Songling Li
Osaka University

Asa Tada
Osaka University

Sumiko Matsuoka
Research Institute for Microbial Diseases, Osaka University

Akemi Arakawa
Osaka University

Kanako Akamatsu
Research Institute for Microbial Diseases, Osaka University

Chikako Ono
Research Institute for Microbial Diseases, Osaka University

Hui Jin
WPI Immunology Frontier Research Center, Osaka University

Kazuki Kishida
WPI Immunology Frontier Research Center, Osaka University

Wataru Nakai
Osaka University https://orcid.org/0000-0001-7350-3125

Masako Kohyama
WPI Immunology Frontier Research Center, Osaka University

Atsushi Nakagawa
Osaka University https://orcid.org/0000-0002-1700-7861

Junichi Takagi

Osaka University https://orcid.org/0000-0002-1219-475X
Yoshiaki Yamagishi
Graduate School of Medicine, Osaka University https://orcid.org/0000-0002-9163-787X
Hironori Nakagami
Osaka University https://orcid.org/0000-0003-4494-3601
Atsushi Kumanogoh
Osaka University https://orcid.org/0000-0003-4749-7117
Yoshiharau Matsuura
Research Institute for Microbial Diseases, Osaka University https://orcid.org/0000-0001-9091-8285
Daron M. Standley
Osaka University
Takayuki Kato
Osaka University https://orcid.org/0000-0002-8879-6685
Masato Okada
Osaka University https://orcid.org/0000-0002-0357-0127
Manabu Fujimoto
Osaka University https://orcid.org/0000-0002-3062-4872

Biological Sciences - Article

Keywords: SARS-CoV-2 variants, anti-receptor binding domain (RBD), N-terminal domain (NTD)

Posted Date: October 20th, 2021

DOI: https://doi.org/10.21203/rs.3.rs-963907/v1

Acquisition of resistance to wild-type spike-immune sera by emerging SARS-CoV-2 variants

Authors:
Yafei Liu[1,2], Noriko Arase[3], Jun-ichi Kishikawa[4], Mika Hirose[4], Songling Li[5], Asa Tada[2], Sumiko Matsuoka[1], Akemi Arakawa[2], Kanako Akamatsu[6], Chikako Ono[7,8], Hui Jin[1], Kazuki Kishida[2], Wataru Nakai[1,2], Masako Kohyama[1,2], Atsushi Nakagawa[9], Junichi Takagi[10], Yoshiaki Yamagishi[11], Hironori Nakagami[12], Atsushi Kumanogoh[13,14], Yoshiharu Matsuura[6,15], Daron M. Standley[5,16], Takayuki Kato[4], Masato Okada[6,16], Manabu Fujimoto[3], Hisashi Arase[1,2,16]*

Affiliations:
[1]Department of Immunochemistry, Research Institute for Microbial Diseases, Osaka University, Osaka, 565-0871, Japan.
[2]Laboratory of Immunochemistry, World Premier International Immunology Frontier Research Centre, Osaka University, Osaka, 565-0871, Japan.
[3]Department of Dermatology, Graduate school of Medicine, Osaka University, Osaka, 565-0871, Japan
[4]Laboratory for CryoEM Structural Biology, Institute for Protein Research, Osaka University, Osaka, 565-0871, Japan.
[5]Dept. Genome Informatics, Research Institute for Microbial Diseases, Osaka University, Osaka, 565-0871, Japan.
[6]Department Oncogene Research, Research Institute for Microbial Diseases, Osaka University, Osaka, 565-0871, Japan.
[7]Laboratory of Virus Control, Center for Infectious Disease Education and Research, Osaka University, Osaka, 565-0871, Japan
[8]Laboratory for Cell Polarity Regulation, RIKEN Center for Biosystems Dynamics Research, Hyogo, 650-0047, Japan
[9]Laboratory for Supramolecular Crystallography, Institute for Protein Research, Osaka University, Osaka, 565-0871, Japan.
[10]Laboratory of Protein Synthesis and Expression, Institute for Protein Research, Osaka University, 3-2 Yamadaoka, Suita, Osaka 565-0871, Japan.
[11]Medical Center for Translational Research, Department of Medical Innovation, Osaka University Hospital, Osaka University, Osaka, 565-0871, Japan.
[12]Department of Health Development and Medicine, Graduate school of Medicine, Osaka University, Osaka, 565-0871, Japan.
[13]Department of Respiratory Medicine and Clinical Immunology, Graduate School of Medicine, Osaka University, Osaka 565-0871, Japan.
[14]Laboratory of Immunopathology, World Premier International Immunology Frontier Research Center, Osaka University, Osaka 565-0871, Japan.
[15]Laboratory of Virus Control, Research Institute for Microbial Diseases, Osaka University, Osaka, 565-0871, Japan
[16]Center for Infectious Disease Education and Research, Osaka University, Osaka, 565-0871, Japan

*Corresponding to: arase@biken.osaka-u.ac.jp

Abstract:

Breakthrough infection is often observed for the SARS-CoV-2 Delta variant, and neutralizing antibody levels are associated with vaccine efficiency[1]. Recent studies revealed that not only anti-receptor binding domain (RBD) antibodies[2] but also antibodies against the N-terminal domain (NTD) play important roles in positively[3,4] or negatively[4-8] controlling SARS-CoV-2 infectivity. Here, we found that the Delta variant completely escaped from anti-NTD neutralizing antibodies, while increasing responsiveness to anti-NTD infectivity-enhancing antibodies. Cryo-EM analysis of the Delta spike revealed that epitopes for anti-NTD neutralizing antibodies are structurally divergent, whereas epitopes for enhancing antibodies are well conserved with wild-type spike protein. Although Pfizer-BioNTech BNT162b2-immune sera neutralized the original Delta variant, when major anti-RBD neutralizing antibody epitopes remaining in the Delta variant were disrupted, some BNT162b2-immune sera not only lost neutralizing activity but became infection-enhanced. The enhanced infectivity disappeared when the Delta NTD was substituted with the wild-type NTD. Sera of mice immunized by Delta spike, but not wild-type spike, consistently neutralized the Delta variant lacking anti-RBD antibody epitopes without enhancing infectivity. Importantly, SARS-CoV-2 variants with similar mutations in the RBD have already emerged according to the GISAID database and their pseudoviruses were resistant to some BNT162b2-immune sera. These findings demonstrate that mutations in the NTD, as well as the RBD, play an important role in antibody escape by SARS-CoV-2. Development of effective vaccines against emerging variants will be necessary, not only to protect against infection, but also to prevent further mutation of SARS-CoV-2.

Introduction

The SARS-CoV-2 Delta variant (B.1.617.2) is highly contagious and is rapidly spreading[9]. Although mRNA vaccines using wild-type spike are quite effective for preventing SARS-CoV-2 infection, as well as severe COVID-19, breakthrough infection is frequently observed for the Delta variant[10,11]. Although anti-RBD antibodies are thought to play a dominant role in vaccine-induced immunity against SARS-CoV-2[2], neutralizing antibodies directed against the NTD are also important for SARS-CoV-2 neutralization[4-8]. Unexpectedly, we and others have found that some anti-NTD antibodies that recognize epitopes distinct from those of anti-NTD neutralizing antibodies, can enhance the infectivity of SARS-CoV-2 by inducing the open form of the RBD, which efficiently binds to host cell receptor ACE2[3,4]. Furthermore, the neutralizing activity of the anti-RBD neutralizing antibodies decreases in the presence of enhancing antibodies[3,4]. Therefore, functions of not only anti-RBD neutralizing antibodies but also anti-NTD neutralizing and infectivity-enhancing antibodies must be considered to understand the infectivity of emerging SARS-CoV-2 variants. In this study, we systemically examined the effect of Delta variant mutations in the NTD and RBD on mRNA vaccine-elicited antibodies and found that unique mutations in the NTD make the Delta variant more resistant to vaccine-elicited antibodies. Furthermore, by examining additional mutations to the Delta variant, we identified emerging SARS-CoV-2 variants resistant to wild-type vaccine-immune sera.

Results

Neutralizing activity of anti-RBD and anti-NTD monoclonal antibodies elicited by wild-type spike against the Delta variant.

We analysed the binding of a series of anti-RBD and anti-NTD antibodies obtained from COVID-19 patients to the spike protein of the Delta variant as well as other major variants: Alpha, Beta, Gamma and Mu (**Fig. 1a**). Because these antibodies were obtained from patients infected in mid-2020, at a time when the SARS-CoV-2 variants had not yet emerged, it is likely that they were

elicited by the wild-type spike protein[2,4-6,12-14]. R346, K417, L452 and E484 are the major anti-RBD neutralizing antibody epitopes often mutated in major variants except for the Alpha variant. The Delta spike has only the L452 mutation among the anti-RBD neutralizing antibody epitopes and thus many anti-RBD neutralizing antibodies still bind to the Delta spike compared to Beta, Gamma and Mu.

Unlike RBD mutations, the NTD mutations of each variant are quite diverse. The Delta variant possess T19R, G142D, E156G, F157del and R158del mutations. Several anti-NTD antibodies that neutralize the SARS-CoV-2 infection have been reported[4-8]. Surprisingly, all 16 anti-NTD neutralizing antibodies we tested failed to recognize the Delta spike, whereas some anti-NTD neutralizing antibodies recognized the NTD of other variants (**Fig. 1a**). Some anti-NTD infectivity-enhancing antibodies[3,4] also lost their binding to the NTD of these variants, but 9 out of 11 anti-NTD infectivity-enhancing antibodies still bound well to the Delta spike at levels comparable with wild-type spike.

Next, we analysed the function of the enhancing and neutralizing antibodies on the Delta variant using pseudovirus bearing either the Delta (Delta pseudovirus) or wild-type spike (wild-type pseudovirus) (**Fig. 1b-1d**). Anti-RBD neutralizing antibodies that bound to the Delta spike completely neutralized the infection of either Delta or wild-type pseudovirus (**Fig. 1c**). Anti-NTD neutralizing antibodies did not neutralize infection by the Delta pseudovirus (**Fig. 1b**). The infectivity enhancement of the Delta pseudovirus by some of the infectivity-enhancing antibodies was more than that of the wild-type pseudovirus (**Fig. 1d**).

We then analyzed the effect of anti-RBD (C144) or anti-NTD (4A8) neutralizing antibodies on the infectivity-enhancing antibodies (COV2-2490) (**Fig. 1e**). The mixture of the neutralizing and enhancing antibodies were serially diluted, and their neutralizing activities against the wild-type or Delta pseudovirus were analyzed. Increased infectivity of the wild-type pseudovirus observed by the anti-NTD infectivity-enhancing antibody was not apparent in the presence of anti-RBD neutralizing antibodies, although the neutralizing activity decreased in the

presence of enhancing antibodies (**Fig. 1e**). Anti-NTD neutralizing antibodies also blocked the increased infectivity of the wild-type pseudovirus induced by infectivity-enhancing antibodies. Surprisingly, the Delta pseudovirus showed strong enhanced infectivity at relatively lower concentrations of a 1:1 mixture of anti-RBD neutralizing and anti-NTD enhancing antibodies (**Fig. 1e**). These data indicated that not only anti-RBD antibodies but also anti-NTD neutralizing antibodies counteract infectivity-enhancing antibody function, whereas the Delta variant completely escaped from anti-NTD neutralizing antibodies while exhibiting increased sensitivity to enhancing antibodies.

Cryo-EM analysis of the Delta spike

We analysed the Delta NTD structure by single particle cryo-EM analysis (3.1 Å resolution) to determine the mechanism by which all anti-NTD neutralizing antibodies failed to recognise the Delta spike, despite the fact that the epitope residues of the anti-NTD neutralizing antibody are conserved in the Delta variant **(Extended Data Fig. 2 and Extended Data Table 1)**. When the NTD models of Delta variant and wild-type spike were compared, the major epitope residues for the enhancing antibody—H64, W66, V213 and R214[3]—were structurally well conserved **(Fig. 2a)**. In contrast, a large conformational change was observed in the residues of anti-NTD neutralizing antibody epitopes. The maximum interatomic distance between the Delta variant and the wild-type was more than 9 Å **(Fig. 2b)**. In the NTD of the Delta variant, the β strands containing four epitope residues—Y144, K147, K150 and W152[5]—were shortened and shifted significantly compared to the wild-type **(Fig. 2a)**. These structural changes were most likely caused by deletion of F157 and R158. As a result, these four residues were quite different from the wild type. R246 and W258 showed large changes compared to the wild-type, and the loop connecting these two residues appeared to be highly flexible. These data indicate that dramatic changes in the structure of the anti-NTD neutralizing antibody epitope residues are responsible for the complete loss of reactivity to anti-NTD neutralizing antibodies against the Delta spike.

The Delta variant is likely to acquire the resistance to the wild-type immune sera.

We analysed the neutralizing activity of twenty sera from healthy individuals fully immunized with Pfizer-BioNTech BNT162b2 mRNA vaccine that use wild-type spike as the immunogen (**Fig. 3a and Extended Data Fig. 3a**). Although most of BNT162b2-immune sera blocked infection of the Delta pseudovirus at high concentration, the neutralizing titre of BNT162b2-immune sera against the Delta pseudovirus decreased significantly compared to wild-type pseudovirus (**Fig. 3b)**, consistent with previous reports[10,11].

Because anti-NTD neutralizing antibodies elicited by wild-type spike immunization do not function against the Delta variant, the neutralizing activity in sera immunized with the wild-type spike used in the current SARS-CoV-2 vaccine is mainly mediated by anti-RBD neutralizing antibodies. K417, N439, E484 and N501 are the major anti-RBD neutralizing antibody epitopes and are often mutated in many variants. Most anti-RBD antibodies recognized the Delta spike with a single additional mutation, but not the Delta spike with mutations at anti-RBD neutralizing antibody epitopes K417N, N439K, E484K and N501Y (Delta ΔRBD-E), although C135, REGN10933 and REGN10987 antibodies still recognized the Delta ΔRBD-E spike **(Fig. 3c)**.

Delta pseudoviruses with an additional single RBD mutation were slightly more resistant to BNT162b2-immune sera, although infection was blocked at the highest concentration of the sera (**Fig. 3d**). Surprisingly, when we analysed the Delta ΔRBD-E pseudovirus, most BNT162b2-immune sera enhanced infectivity in a dose-dependent manner at relatively low concentrations, but showed weak neutralization only at the highest concentration of the sera **(Fig. 3e and Extended Data Fig. 3b)**. In particular, PFZ2 greatly enhanced the infectivity at relatively low serum concentration. PFZ5 showed only enhancement. On the other hand, PFZ4 effectively neutralized the Delta ΔRBD-E pseudovirus, but the neutralizing titres of PFZ4 against the wild type and Delta variant were not particularly high compared to the others **(Fig. 3e)**.

Similar unique neutralizing activity of BNT162b2-immune sera against the Delta ΔRBD-

E pseudovirus—enhancing infection at low concentrations and neutralizing it at high concentrations—was also observed for the Delta pseudovirus by a mixture of the neutralizing and enhancing antibodies **(Fig. 1e)**. The Delta ΔRBD-E pseudovirus in which the NTD was substituted with wild-type NTD did not show enhanced infectivity by BNT162b2-immune sera **(Fig. 3e and 3f, Extended Data Fig. 3b)**. These data indicate that large the conformational change of NTD by the Delta mutations makes the virus more sensitive to anti-NTD antibodies in BNT162b2-immune sera and that the effect of the enhanced antibodies becomes evident when anti-RBD neutralizing antibodies become less effective by further mutations in the RBD.

Emergence of SARS-CoV-2 variants resistance to wild-type spike-immune sera

The Delta variant has already acquired large numbers of additional mutations in the RBD, some of which occur in epitopes for anti-RBD neutralizing antibodies and are increasing **(Extended Data Fig. 4a and 4b)**. Not only the Delta variants with single mutations but also more than two additional mutations in the RBD are increasing in the GISAID database **(Extended Data Fig. 4c)**. Several Delta variants with mutations at both E484Q and K417N, also used for Delta ΔRBD-E, were registered late September, 2021 **(Extended Data Fig. 4c and 4d)**. Delta spikes with E484K plus K417N (Delta 2+) mutations as well as E484Q plus K417N mutations were not recognized by most anti-RBD neutralizing antibodies **(Fig. 3c)**. Furthermore, the Delta 2+ pseudovirus was resistant to BNT162b2-immune sera similar to the Delta ΔRBD-E pseudovirus, and it showed enhanced infectivity by some immune sera **(Fig. 3g)**.

The Mu variant, a variant of interest (VOI), possess R346K, E484K and N501Y mutations in the RBD; approximately 10% of recent Mu variants exhibit the K417N mutation (Mu 1+), and a few Mu variants exhibit L452R (Mu 2+), K444R or Q498R mutation in addition to K417N mutation **(Extended Data Fig. 5a)**. The Mu 2+ spikes were not recognized by most anti-RBD neutralizing antibodies **(Extended Data Fig. 5b)**. Although the infectivity of the Mu pseudovirus was neutralized by BNT162b2-immune sera, the neutralizing activity against Mu 1+

and Mu 2+ pseudovirus decreased and some sera did not neutralize at all, even at high concentrations and showed enhanced infectivity at relatively low concentrations, similar to the Delta ΔRBD-E variant **(Fig. 3h and Extended Data Fig. 5c)**. Most anti-NTD neutralizing antibodies failed to recognize the Mu NTD possessing several unique mutations, although not so complete compared to the Delta NTD **(Fig. 1a)**. These data suggest that the effect of infectivity-enhancing antibodies become evident when the SARS-CoV-2 variants with large conformational change at the NTD acquires further mutations at anti-RBD neutralizing epitopes.

Sera from the Delta spike immunized mice do not show enhanced infectivity against Delta ΔRBD-E pseudovirus.

The enhanced infectivity of the Delta ΔRBD-E pseudovirus by some BNT162b2-immune sera appears to be caused by the decreased neutralizing antibody titre of anti-NTD and anti-RBD neutralizing antibodies against Delta ΔRBD-E pseudovirus. High neutralizing antibody titres against the Delta variants will be obtained by immunizing with the Delta spike. To test this possibility, we immunized mice with B16F10 mouse melanoma cells transiently transfected with wild-type or Delta spike protein **(Fig. 4a)**. All immunized mice effectively produced antibodies against spike protein **(Extended Data Fig. 6)**. The wild-type spike immunized sera neutralized wild-type pseudovirus well, whereas the neutralizing effect against the Delta pseudovirus decreased similar to BNT162b2-immune sera **(Fig. 4b and 4c)**. In contrast, Delta spike immunized sera neutralized both wild-type and Delta pseudovirus well. Just one mouse produced antibodies that neutralized the Delta pseudovirus better than wild-type pseudovirus. When we analysed the Delta ΔRBD-E pseudovirus, some sera from wild-type spike immunized mice showed enhanced infectivity in a dose dependent manner at relatively low concentrations of sera, similar to some BNT162b2-immune sera **(Fig. 4d and 4e)**. In particular, the #w1 mouse serum showed enhanced infectivity at any concentration, although the same serum neutralized the wild-type pseudovirus well. In contrast, the enhanced infectivity by immunized sera was not observed

when the Delta spike was used for immunization. Sera from the Delta-spike immunized mice did not exhibit enhanced infectivity at any concentration of sera. These data suggest that vaccines containing the Delta spike are superior to control Delta subvariants that may emerge in the future.

Discussion

Many anti-NTD neutralizing antibodies failed to bind to the Alpha, Beta, Gamma and Mu variants, although less completely than the Delta variant. This suggested that anti-NTD neutralizing antibodies play an important role in the protection against SARS-CoV-2 infection and thus these variants have acquired NTD mutations to escape from these antibodies. The infectivity-enhancing antibodies bind to a specific site on the NTD, inducing the open form of the RBD, which increases the affinity of spike protein to ACE2[3]. The enhancing antibody epitopes are relatively conserved among the major SARS-CoV-2 variants and the Delta variant is more sensitive to enhancing antibodies. Recent studies demonstrated that Fc receptors are required for SARS-CoV-2 protection by both anti-RBD and anti-NTD neutralizing antibodies *in vivo*[6,15,16], indicating that the effector function of antibodies is important for antibody-mediated SARS-CoV-2 protection. Therefore, enhancing antibodies might also work for SARS-CoV-2 protection through Fc receptors *in vivo*, depending on the antibody subclass, concentration and affinity to the NTD.

Several BNT162b2 immune sera showed neutralizing activity against the Delta ΔRBD-E pseudovirus at a 1:10 dilution, but conversely increased infectivity at 1:31.6 dilution. Similar neutralizing activities were observed for the Delta pseudovirus but not the wild-type pseudovirus when neutralizing and enhancing antibodies were mixed. Since the effect of anti-NTD infectivity-enhancing antibodies is affected by the concentration of anti-RBD neutralizing antibodies[3,4], the effect of infectivity-enhancing antibodies in BNT162b2 immune sera is likely to be more pronounced when the concentration of anti-RBD neutralizing antibodies falls below a certain threshold. Because the neutralizing antibody titres are different among individuals and gradually decrease after immunization[17,18], the effect of infectivity-enhancing antibodies may become more

evident some time after immunization, as in the case of diluted sera. On the other hand, one BNT162b2 immune serum neutralized the Delta ΔRBD-E pseudovirus well. The delicate balance of antibody titre, affinity, subclass, or epitope between neutralizing and enhancing antibodies all influence the infectivity in sera. The Delta variants with K417N and E484Q mutations and the Mu variants with K417N and L452R mutations have recently emerged according to the GISAID database. The Delta pseudovirus with K417N and E484K mutations showed enhanced infectivity by the BNT162b2 immune sera, similar to the Delta ΔRBD-E pseudovirus. Mu 1+ or Mu 2+ pseudovirus were also resistant to the BNT162b2 immune sera. Considering of their resistance to the wild-type spike immune sera, monitoring these variants are important to prevent their spread.

Neutralization antibody titres are associated with vaccine efficiencies[1], although loss of neutralizing activity does not always mean that immunization is ineffective. Immunization by Delta spike induces antibodies that neutralize not only the Delta variant but also wild-type and the Delta ΔRBD-E pseudovirus without enhancing the infectivity, indicating that mRNA vaccines expressing the Delta spike will be effective for controlling the emerging Delta variant. Epitopes of the enhancing antibodies, not neutralizing antibodies, are relatively conserved among most SARS-CoV-2 variants, suggesting that additional immunization of the variant-derived spike protein may boost enhancing antibodies more than the neutralizing antibodies in individuals who were previously infected with wild-type SARS-CoV-2 or immunized with vaccines composed of wild-type spike protein[19]. Development of vaccines that induce antibodies that effectively neutralize the emerging SARS-CoV-2 variants without enhancing the infectivity may need to be considered.

Methods

Cell lines

HEK293T cells (RIKEN Cell Bank) and B16F10 melanoma cells (National Institute of Biomedical Innovation) were cultured in DMEM (Nacalai, Japan) supplemented with 10% FBS

(Biological Industries, USA), penicillin (100 U/mL), and streptomycin (100 μg/mL) (Nacalai, Japan) and cultured at 37°C in 5% CO_2. The Expi293 cells (Thermo) were cultured with the Expi293 medium. The cells were routinely checked for mycoplasma contamination. ACE2-stably transfected HEK293 cells (HEK293T-ACE2-transfectants) were reported previously[3].

Human samples

The collection and use of BNT162b2-immune sera were approved by Osaka University Hospital (20522-3). Written informed consent was obtained from the participants according to the relevant guidelines of the institutional review board. All sera were collected from 26-65 years old healthy individuals three weeks after immunization with two cycles of 30 μg of BNT162b2 mRNA vaccine.

Plasmid construction

The SARS-CoV-2 spike gene (NC_045512.2) was prepared by gene synthesis (IDT). The sequences encoding the spike protein lacking the C-terminal 19 amino acids (amino acids 1–1254) were cloned into the pME18S expression vector. A series of mutants and the Alpha (ΔV70, ΔH69, ΔY144, N501Y, D614G, A570D, T716I, P681H, S982A, D1118H), Beta (L18F, D80A, D215G, ΔL242, ΔA243, ΔL244, K417N, E484K, N501Y, D614G, A701V), Gamma (L18F, T20N, P26S, D138Y, R190S, K417T, N501Y, E484K, D614G, H655Y, T1027I, V1176F), Delta (T19R, G142D, E156G, ΔF157, ΔR158, L452R, T478K, D614G, P681R, D950N) and Mu (T95I, Y144T, Y145S, insertion 145N, R346K, E484K, N501Y, D614G, P681H, D950N) variants were prepared from wild-type SARS-CoV-2 spike using the QuickChange Lighting Multi Site-directed Mutagenesis kit (Agilent). Additional RBD mutations were introduced into the Delta spike also using the QuickChange Lighting Multi Site-directed Mutagenesis kit (Agilent). The primers for mutagenesis were designed on Agilent's website (https://www.agilent.com/store/primerDesignProgram.jsp). For Cryo-EM analysis, the sequence

encoding the spike protein's extracellular domain with a foldon and His-tag at the C-terminus[20] was cloned into a pcDNA3.4 expression vector containing the SLAM signal sequence. Also, mutations D614G, R686G R687S R689G, K986P, and V987P were introduced using a Quick change multi-mutagenesis kit (Agilent) for stabilization of recombinant spike protein[21]. The DNA sequences of these constructs were confirmed by sequencing (ABI3130xl).

Transfection

A pME18S expression plasmid containing the full-length or subunit spike protein was transiently transfected into HEK293T cells using PEI max (Polysciences); the pMx-GFP expression plasmid was used as the marker of transfected cells.

Anti-spike monoclonal antibodies from COVID-19 patients

The variable regions of anti-SARS-CoV-2 spike antibodies from COVID-19 patients were synthesized according to the published sequence[2,4-6,12-14]. Variable region sequences of some antibodies were obtained from the CoV-AbDab database (http://opig.stats.ox.ac.uk/webapps/covabdab/). The cDNA of the variable regions of the heavy chain and light chain were cloned into a pCAGGS vector containing sequences that encode the human IgG1 or kappa constant region. The pCAGGS vectors containing sequences encoding the immunoglobulin heavy chain and light chain were co-transfected into Expi293 (Thermo) cells, and the cell culture supernatants were collected according to the manufacturer's protocols. Recombinant IgG was purified from the culture supernatants using protein A Sepharose (GE healthcare). The concentration of purified IgG was measured at OD280.

Antibodies and recombinant proteins

Allophycocyanin (APC)-conjugated donkey anti-mouse IgG Fc fragment antibody and APC-conjugated anti-human IgG Fc fragment specific antibody (Jackson ImmunoResearch, USA) were

used. The pcDNA3.4 expression vector containing the sequence that encodes the His-tagged extracellular domain of the spike protein was transfected into Expi293 cells and the His-tagged spike protein produced in the culture supernatants was then purified with a Talon resin (Clontech).

Immunization of mice

B16F10 cells were transfected with WT spike protein or Delta spike protein by PEI as described above. 48 hours later, B16F10 cells were washed twice with PBS, and then the cells were collected and frozen and thawed. Balb/c female mice (7-weeks-old females) were purchased from SLC. Two groups of five mice (n = 5) were subcutaneously immunized with $1x10^7$ B16F10 transfectants in the presence of complete Freund's adjuvant (CFA). Serum samples were collected three weeks after the immunization.

Flow cytometric analysis of antibodies

Plasmids expressing the full-length SARS-CoV-2 spike protein, Flag-NTD-PILR-TM and Flag-RBD-PILR-TM were co-transfected with the GFP vector into HEK293T cells. The transfectants were incubated with the mAbs, followed by APC-conjugated anti-human IgG Ab. The antibodies bound to the stained cells were then analysed using a flow cytometer (Attune™, Thermo; FACSCelesta BD bioscience). Antibodies binding to the GFP-positive cells were shown in the figures using FlowJo software (BD bioscience).

SARS-CoV-2 spike-pseudotyped virus infection assay

The HEK293T cells were transiently transfected with expression plasmids for the SARS-CoV-2 spike protein lacking the C-terminal 19 amino acids [22,23]. At 24 hours post-transfection, VSV-G-deficient VSV carrying a Luciferase gene complemented in *trans* with the VSV-G protein was added for incubation for 2 hours. The cells were then carefully washed with DMEM media without FBS and incubated with DMEM with FBS at 37°C in 5% CO_2 for 48 hours. The

supernatant containing the pseudotyped SARS-CoV-2 virions was harvested and aliquoted before storage at −80°C. To determine the virus titres of the pseudovirus, 1× 10^4 HEK293T-ACE2-transfectants were mixed with the pseudovirus for 20 hours at 37 °C in 5% CO_2 in a 384-well plate (Greiner, Germany). Luciferase activity was measured using a ONE-Glo™ luciferase assay (Promega, USA) according to the manufacturer's instructions. The signals were measured by a luminescence plate reader (TriStar LB94, Berthold Technologies, Germany) **(Extended Data Fig. 1)**. For the neutralization assay, 5 µl pseudovirus was mixed with equal volume of sera or monoclonal antibodies at the concentrations indicated in the figure. The mixture was added to 20 µl of 1× 10^4 HEK293T-ACE2-transfectants. To calculate % neutralization, the relative luminescence units of the virus control wells (pseudovirus only) were subtracted from those of the sample wells, and the subtracted values were divided by those of the virus control wells. The PRNT50 neutralization titres for vaccinated sera were determined using 3-parameter nonlinear regression curve (GraphPad Prism). If the PRNT50 titre was less than 1:10, it was defined as 0.

Cryo-EM data collection

A 2.5 µl protein solution of the spike protein (2.2 mg/ml) was applied onto the cryo-grid and frozen in liquid ethane using a Vitrobot IV (Thermo Fisher Scientific, USA, 4°C and 100% humidity). Quantifoil Au R0.6/1.0 holey carbon grids were used for the grid preparation. Data collection of the sample was carried out on a Titan Krios (Thermo Fisher Scientific, USA) equipped with a thermal field emission electron gun operated at 300 kV, an energy filter with a 20 eV slit width and a bioquantum K3 direct electron detection camera (Gatan, USA) (Figure S4). For automated data acquisition, SerialEM software was used to collect cryo-EM image data. Movie frames were recorded using the K3 camera at a calibrated magnification of × 81,000 corresponding to a pixel size of 0.88 Å with a setting defocus range from −0.8 to −2.0 µm. The data were collected with a total exposure of 3 s fractionated into 62 frames, with a total dose of ~

60 electrons Å^2 in counting mode. A total number of movies were collected; 15,000 for the spike protein.

Image processing and 3D reconstruction

All of image processes were carried out on cryoSPARC software[24]. After motion correction of movies and CTF parameter estimation, the particles were automatically picked using Topaz software[25]. The detailed information is summarized in **Extended Data Table 1**. The picked particles were extracted into a box of 360 × 360 pixels. After particle extraction, the particles were applied to two rounds of heterogenous refinement with C1 symmetry. The selected particles (735,623 particles) were applied to two rounds of *ab-initio* reconstruction into three classes with C1 symmetry. In the first and second rounds of ab-initio reconstruction, the class similarity parameter, 0.1 and 0.8, was used, respectively. After that, the selected 147,497 particles were further used as non-uniform refinement with optimizing per-particle defocus. As the result, the density map for the spike protein was obtained at 3.16 Å resolution. Local resolution of the obtained maps was estimated by Local resolution estimation job on cryoSPARC.

Model building and refinement

To generate the atomic model for the spike protein, the structure of NTD of Delta variant was predicted using AlphaFold2[26]. The structure of the NTD was predicted in CASP14 mode without template. For other domains, the model from previous study (PDBID; 7JJI) was used. These structures were fitted into the density map as rigid body using UCSF chimera[27]. The initial model was extensively manually corrected residue by residue in COOT[28] in terms of especially side-chain conformations. The corrected model was refined by the phenix.real_space_refine program[29] with secondary structure and Ramachandran restraints, then the resulting model was manually checked by COOT. This iterative process was performed for several rounds to correct remaining errors until the model was in good agreement with geometry, as reflected by the MolProbity score

of 2.07[30]. For model validation against over-fitting, the built models were used for calculation of FSC curves against the final density map used for model building by phenix.refine program. The statistics of the obtained maps and the atomic model were summarized in **Extended Data Table 1**. Cα displacement between the wild-type and the Delta NTD shown in **Fig. 2b** was calculated by UCSF chimera.

Data and statistical analysis

FlowJo version 10.7 (BD Biosciences, USA) was used to analyse the flow cytometry data, and Graphpad Prism version 7.0e was used for graph generation and statistical analysis.

Data availability

Cryo-EM density maps for the SARS-CoV-2 Delta spike protein were deposited at the EMDB under accession code EMD-31731. A molecular model of the SARS-CoV-2 Delta spike protein fitted to Cryo-EM data were deposited to PDB under accession code 7V5W. The data that support the findings of this study are available from the Lead Contact on request.

References

1. Khoury, D. S. *et al.* Neutralizing antibody levels are highly predictive of immune protection from symptomatic SARS-CoV-2 infection. *Nat Med* **27**, 1205-1211, (2021).
2. Robbiani, D. F. *et al.* Convergent antibody responses to SARS-CoV-2 in convalescent individuals. *Nature* **584**, 437-442, (2020).
3. Liu, Y. *et al.* An infectivity-enhancing site on the SARS-CoV-2 spike protein targeted by antibodies. *Cell* **184**, 3452-3466 e3418, (2021).
4. Li, D. *et al.* In vitro and in vivo functions of SARS-CoV-2 infection-enhancing and neutralizing antibodies. *Cell* **184**, 4203-4219 e4232, (2021).
5. Chi, X. *et al.* A neutralizing human antibody binds to the N-terminal domain of the Spike

protein of SARS-CoV-2. *Science* **369**, 650-655, (2020).

6. Suryadevara, N. *et al.* Neutralizing and protective human monoclonal antibodies recognizing the N-terminal domain of the SARS-CoV-2 spike protein. *Cell* **184**, 2316-2331 e2315, (2021).
7. Voss, W. N. *et al.* Prevalent, protective, and convergent IgG recognition of SARS-CoV-2 non-RBD spike epitopes. *Science* **372**, 1108-1112, (2021).
8. Liu, L. *et al.* Potent neutralizing antibodies against multiple epitopes on SARS-CoV-2 spike. *Nature* **584**, 450-456, (2020).
9. Callaway, E. Delta coronavirus variant: scientists brace for impact. *Nature* **595**, 17-18, (2021).
10. Liu, C. *et al.* Reduced neutralization of SARS-CoV-2 B.1.617 by vaccine and convalescent serum. *Cell* **184**, 4220-4236 e4213, (2021).
11. Planas, D. *et al.* Reduced sensitivity of SARS-CoV-2 variant Delta to antibody neutralization. *Nature* **596**, 276-280, (2021).
12. Brouwer, P. J. M. *et al.* Potent neutralizing antibodies from COVID-19 patients define multiple targets of vulnerability. *Science* **369**, 643-650, (2020).
13. Zost, S. J. *et al.* Rapid isolation and profiling of a diverse panel of human monoclonal antibodies targeting the SARS-CoV-2 spike protein. *Nat Med* **26**, 1422-1427, (2020).
14. Baum, A. *et al.* Antibody cocktail to SARS-CoV-2 spike protein prevents rapid mutational escape seen with individual antibodies. *Science* **369**, 1014-1018, (2020).
15. Winkler, E. S. *et al.* Human neutralizing antibodies against SARS-CoV-2 require intact Fc effector functions for optimal therapeutic protection. *Cell* **184**, 1804-1820 e1816, (2021).
16. Schafer, A. *et al.* Antibody potency, effector function, and combinations in protection and therapy for SARS-CoV-2 infection in vivo. *J Exp Med* **218**, (2021).
17. Doria-Rose, N. *et al.* Antibody Persistence through 6 Months after the Second Dose of mRNA-1273 Vaccine for Covid-19. *N Engl J Med* **384**, 2259-2261, (2021).

18. Widge, A. T. *et al.* Durability of Responses after SARS-CoV-2 mRNA-1273 Vaccination. *N Engl J Med* **384**, 80-82, (2021).

19. Chakradhar, S. Updated, augmented vaccines compete with original antigenic sin. *Nat Med* **21**, 540-541, (2015).

20. Cai, Y. *et al.* Distinct conformational states of SARS-CoV-2 spike protein. *Science* **369**, 1586-1592, (2020).

21. Yurkovetskiy, L. *et al.* Structural and Functional Analysis of the D614G SARS-CoV-2 Spike Protein Variant. *Cell* **183**, 739-751 e738, (2020).

22. Johnson, M. C. *et al.* Optimized Pseudotyping Conditions for the SARS-COV-2 Spike Glycoprotein. *J Virol* **94**, e01062-01020, (2020).

23. Hu, J. *et al.* Development of cell-based pseudovirus entry assay to identify potential viral entry inhibitors and neutralizing antibodies against SARS-CoV-2. *Genes Dis* **7**, 551-557, (2020).

24. Punjani, A., Rubinstein, J. L., Fleet, D. J. & Brubaker, M. A. cryoSPARC: algorithms for rapid unsupervised cryo-EM structure determination. *Nat Methods* **14**, 290-296, (2017).

25. Bepler, T. *et al.* Positive-unlabeled convolutional neural networks for particle picking in cryo-electron micrographs. *Nat Methods* **16**, 1153-1160, (2019).

26. Jumper, J. *et al.* Highly accurate protein structure prediction with AlphaFold. *Nature* 10.1038/s41586-021-03819-2, (2021).

27. Pettersen, E. F. *et al.* UCSF Chimera--a visualization system for exploratory research and analysis. *J Comput Chem* **25**, 1605-1612, (2004).

28. Emsley, P., Lohkamp, B., Scott, W. G. & Cowtan, K. Features and development of Coot. *Acta Crystallogr D Biol Crystallogr* **66**, 486-501, (2010).

29. Liebschner, D. *et al.* Macromolecular structure determination using X-rays, neutrons and electrons: recent developments in Phenix. *Acta Crystallogr D Struct Biol* **75**, 861-877, (2019).

30. Williams, C. J. *et al.* MolProbity: More and better reference data for improved all-atom structure validation. *Protein Sci* **27**, 293-315, (2018).

Acknowledgments

We would like to thank Yumi Inaba for her administrative assistance. We would like to thank technical assistance of the members of the Department of Dermatology, Osaka University, Osaka, Japan. This work was supported by JSPS KAKENHI under Grant Numbers JP18H05279 and JP19H03478 (HA), MEXT KAKENHI under Grant Number JP19H04808 (HA), Japan Agency for Medical Research and Development (AMED) under Grant Numbers, JP20fk0108542 (HA), JP20nf0101623 (HN, HA), 20fk0108403h (HA), JP20am0101108 (DMS), JP21am0101072 (TK, AN, BINDS support number 2630) and Japan Science and Technology Agency (JST) (Moonshot R&D) JPMJMS2025 (YM), and Panasonic Corporation (HA, YM).

Author contributions

Y.L., Y.M., A.N., J.T., D.M.S., T.K., M.O., M.F., H.A. designed the experiments. Y.L., J.K., M.H., A.T, S.M., A.A., K.A., C.O., H.J., K.K., W.N., performed the experiments. N.A., A.K., H.N., Y.Y., M.F. collected vaccine sera. J.K., S.L., D.M.S, T.K., H.A. constructed a model of NTD spike. Y.L., N.A., J.K, M.K., D.M.S, H.A. wrote the manuscript. All authors read, edited, and approved the manuscript.

Competing interests

Osaka University has filed a patent application for the enhancing antibodies. HA and YL are listed as inventors. HA is a stockholder of HuLA immune Inc.

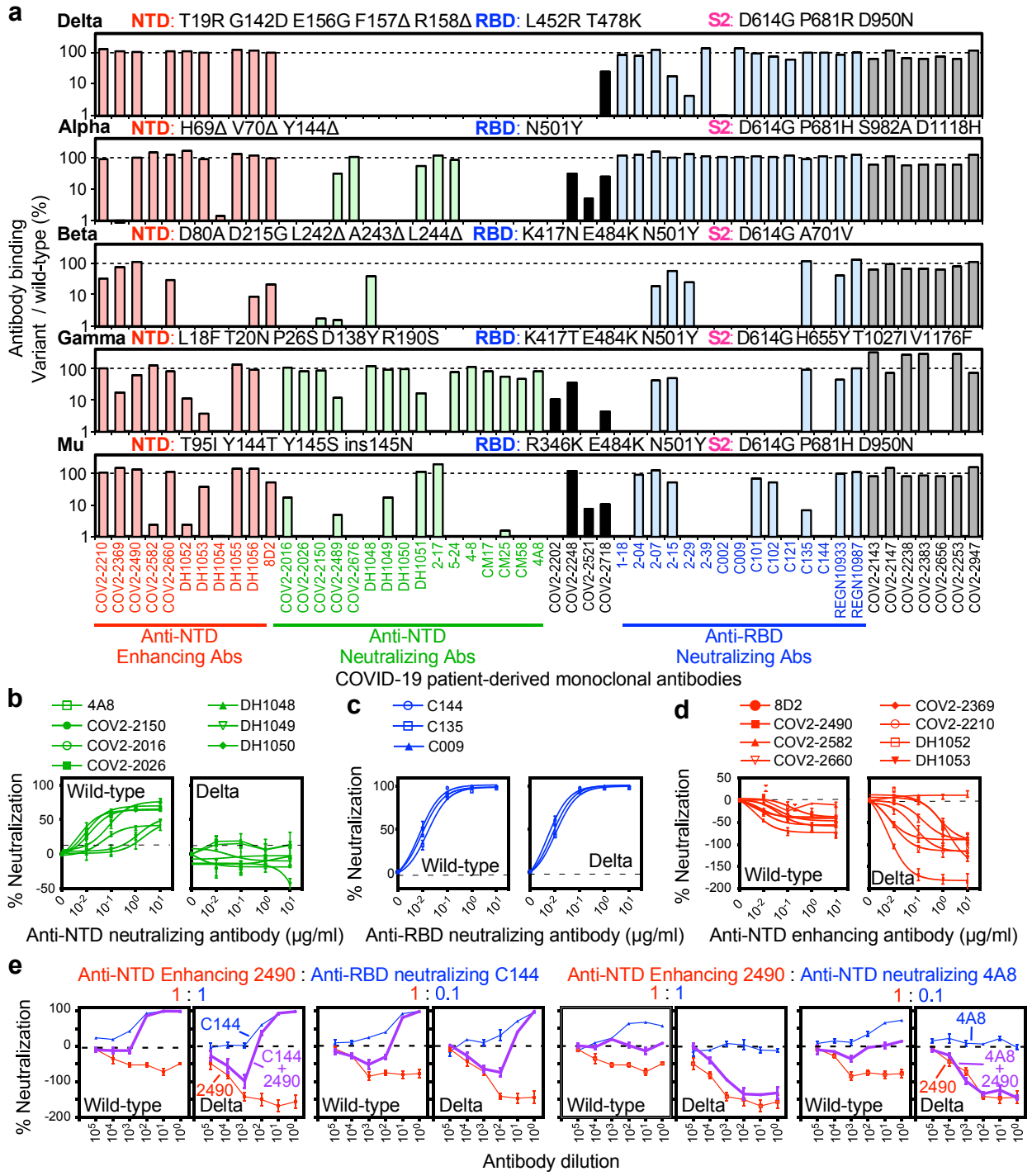

Fig. 1. Neutralizing and enhancing effects against the wild-type and Delta spike pseudovirus by anti-spike monoclonal antibodies from COVID-19-patients.

a, Binding of anti-NTD enhancing (red), anti-NTD neutralizing (green), anti-NTD non-functional (black), anti-RBD neutralizing (blue) and anti-S2 (grey) antibodies (1 μg/ml) to the Delta, Alpha, Beta, Gamma and Mu spikes compared to the wild-type spike. **b-d,** Neutralizing activity of the anti-NTD neutralizing (**b**), anti-RBD neutralizing (**c**) and anti-NTD enhancing (**d**) antibodies against the wild-type or Delta pseudovirus. **e,** Anti-NTD enhancing antibodies (COV2-2490 (2490), 10 μg/ml) were mixed with anti-RBD (C144) or anti-NTD (4A8) neutralizing antibodies at 1:1 or 1:0.1 ratio. Neutralizing activities against the wild-type or Delta pseudovirus of the serially diluted mixed (purple), enhancing (red) or neutralizing (blue) antibodies. A negative value for % neutralization indicates enhanced infectivity (**b, c, d, e**). The data from quadruplicates are presented as mean ± SEM. The representative data from three independent experiments are shown.

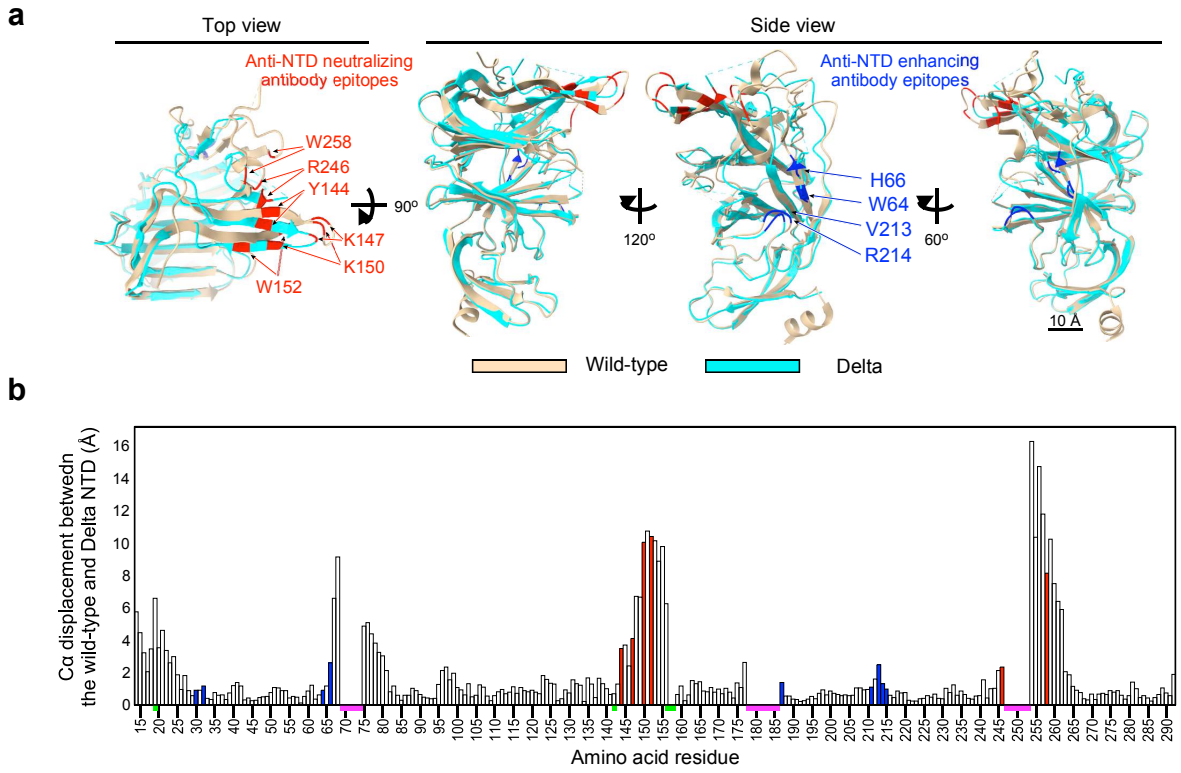

Fig. 2. Cryo-EM analysis of the Delta NTD mutations

a, Structure of the Delta NTD (light blue) analysed by the Cryo-EM were superimposed with the wild-type NTD (light brown, PDB: 7LY3). Anti-NTD enhancing antibody epitopes: blue, anti-NTD neutralizing antibody epitopes: red. **b,** Cα displacement between the wild-type and the Delta NTD. Anti-NTD enhancing antibody epitopes: blue, anti-NTD neutralizing antibody epitopes: red. Structures not determined: magenta, mutations in the Delta NTD: green.

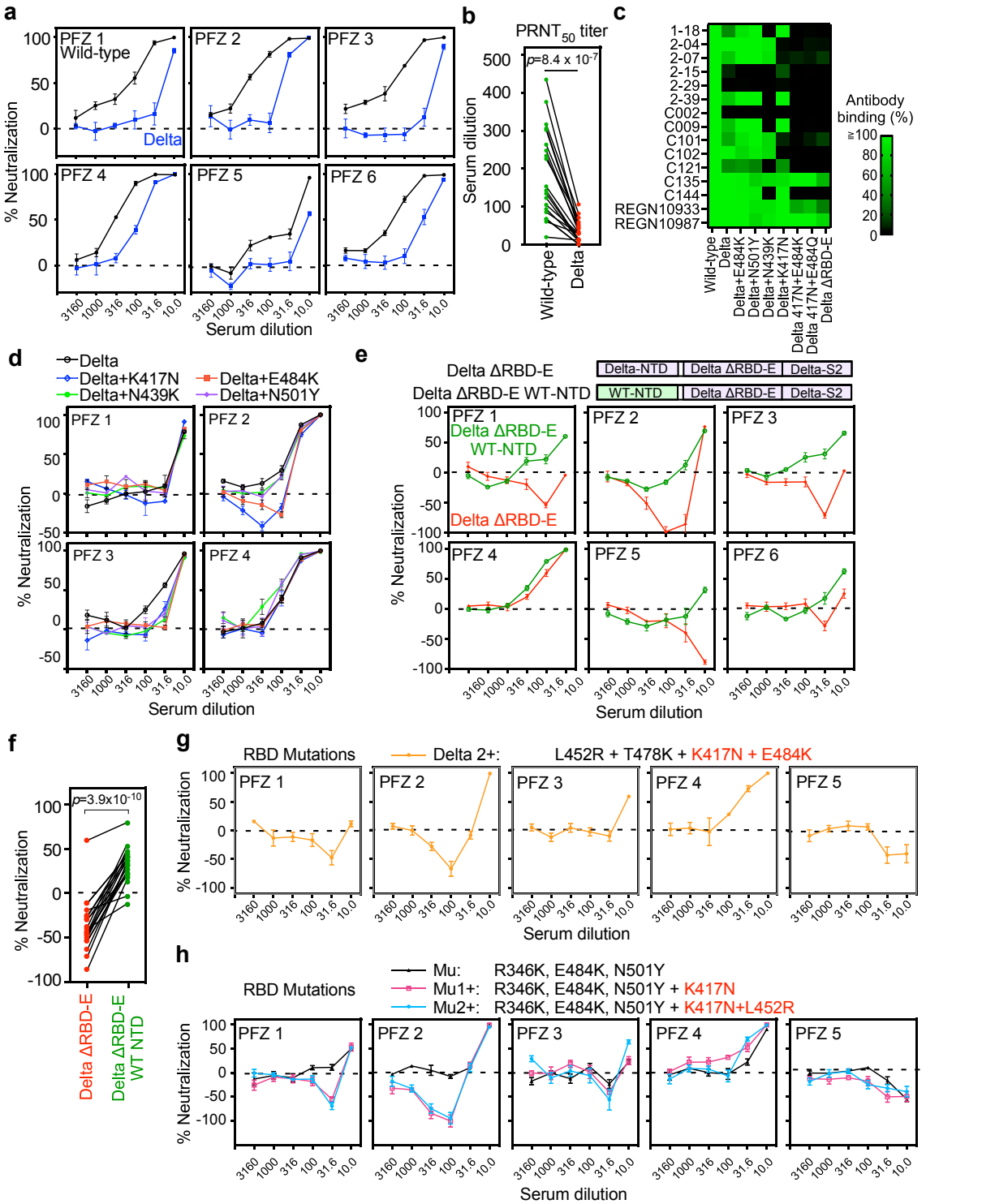

Fig. 3. Acquisition of resistance to wild-type spike-immune sera by SARS-CoV-2 variants.
a, e, Neutralizing activity of the representative six out of twenty BNT162b2-immune sera against the wild-type and the Delta pseudovirus **(a)**, Delta ΔRBD-E and Delta ΔRBD-E with wild-type NTD (WT-NTD) pseudovirus **(e)**, **b,** PRNT50 titres of the twenty BNT162b2-immune sera. **c,** Anti-RBD antibody binding to the Delta spike with additional mutations at the RBD compared with the wild-type spike. **d,** Neutralizing activity of the BNT162b2-immune sera against the Delta pseudoviruses with single RBD mutations. **f,** Neutralizing activity of 31.6 times diluted twenty BNT162b2-immune sera. **g, h,**. Neutralizing activity of the representative five BNT162b2-immune sera against the Delta **(g)** or Mu **(h)** pseudovirus with additional RBD mutations. *p* values were determined by paired t-test. Negative values for % neutralization indicate enhanced infectivity (**a, d, e, f, g, h**). The data from quadruplicates are presented as mean ± SEM. The representative data from three independent experiments are shown.

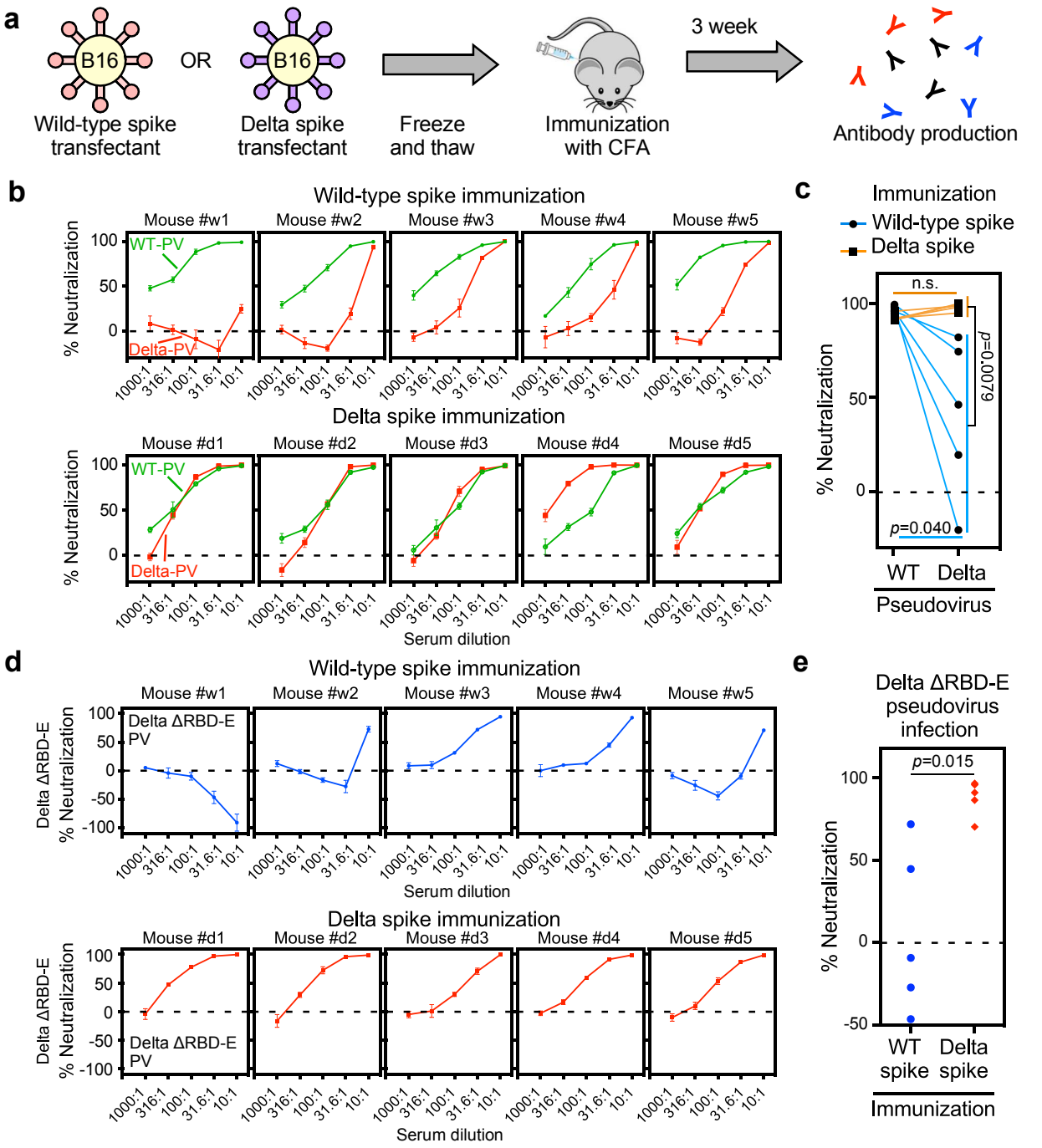

Fig. 4. Sera from delta spike-immunized mice do not show enhanced infectivity

a, The wild-type or Delta spike were immunized to the mice with complete Freund's adjuvant (CFA). **b,** Neutralizing activity against the wild-type (green) or Delta (red) pseudovirus (PV) by sera from the wild-type spike (upper column) or Delta spike (lower column) spike-immunized mice. **c,** Neutralizing activity against the wild-type and Delta pseudovirus by 31.6 times-diluted sera from wild-type (light blue line) or Delta (orange line) spike-immunized mice. **d,** Neutralizing activity against the Delta ΔRBD-E pseudovirus by sera from the wild-type spike (upper column, blue) or Delta spike (lower column, red) immunized mice. **e,** Neutralizing activity against the Delta ΔRBD-E pseudovirus by the 31.6 times-diluted sera from the wild-type spike (blue) or Delta spike (red) immunized mice. n.s.: not statistical significance, *p* value was determined by t-test. Negative values for % neutralization indicate enhanced infectivity (**b, c, d, e**). All data from quadruplicates are presented as mean ± SEM.

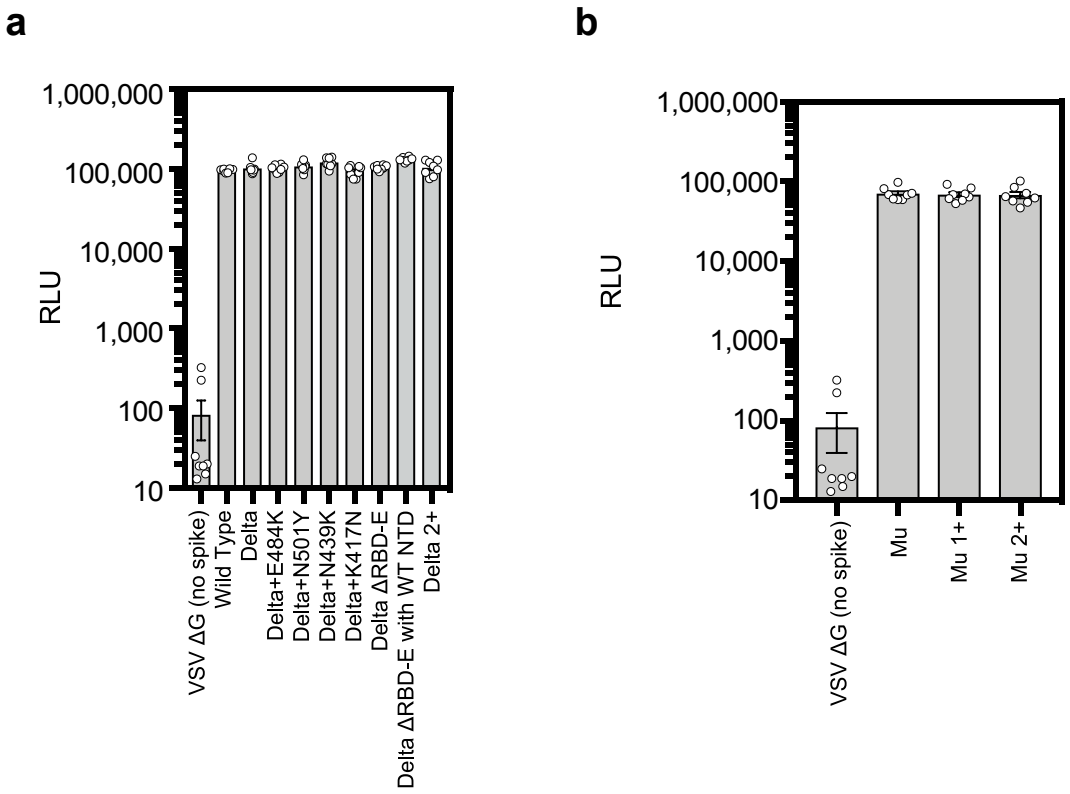

Extended Data Fig. 1 Viral titres of pseudotyped viruses

a, b, The viral titres for the Delta spike **(a)** or Mu spike **(b)** psudoviruses were measured by infection of ACE2-transfected HEK293T cells as described in Methods.

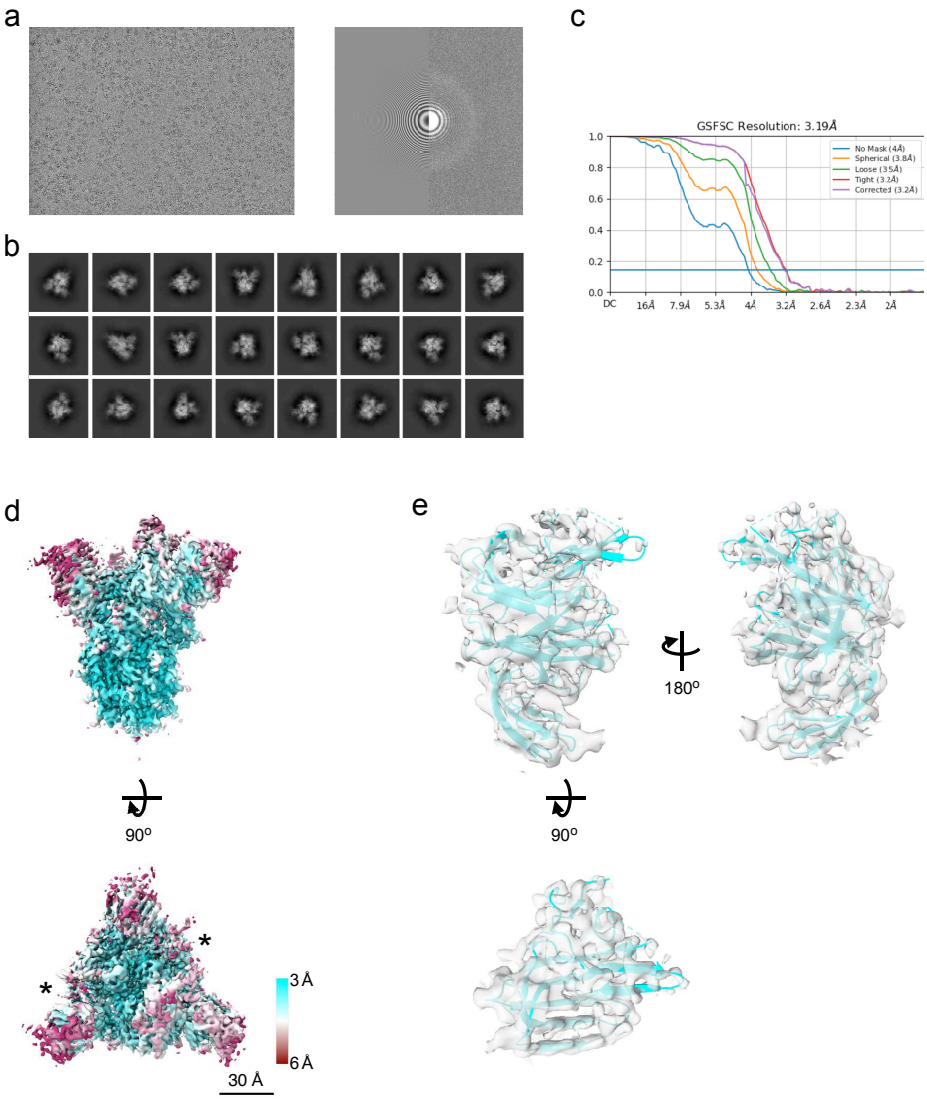

Extended Data Fig. 2 Cryo-EM density map of spike of SARS-CoV-2 Delta variant.
a, A representative micrographs (left), CTF estimation of a micrograph on left panel (right). **b,** Typical 2D class averages. **c,** The GS-FSC curves for the obtained map from cryoSPARC software are shown. Blue flat line indicates FSC=0.143 criteria. **d,** The density map of spike protein from Delta strain (EMDBID: 31731). The map is coloured with local resolution. Asterisks indicate the up form of RBDs. Scale bars are 30 Å. **e,** The structure of NTD from spike protein of Delta variant. The density map and the model are shown as semi-transparent surface and cartoon, respectively (PDBID: 7V5W).

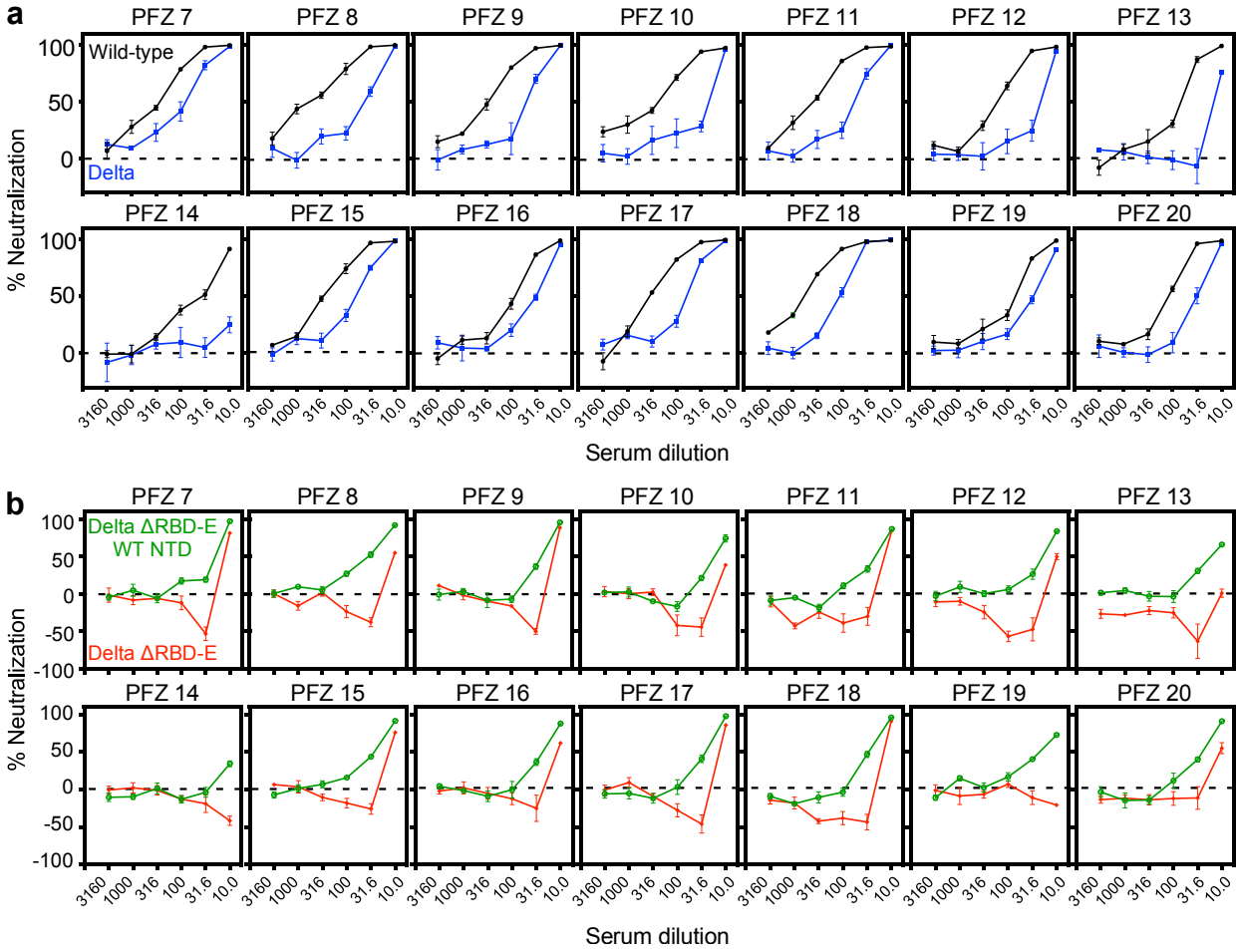

Extended Data Fig. 3. Acquisition of resistance to wild-type spike-immune sera by SARS-CoV-2 Delta variant by additional mutations at RBD.

a, Neutralizing activity of the 14 out of twenty BNT162b2-immune sera, not shown in **Fig. 3a**, against the wild-type (black) and the Delta (blue) pseudovirus. **b,** Neutralizing activity of the 14 out of twenty BNT162b2-immune sera, not shown in **Fig. 3e**, against the pseudovirus with Delta ΔRBD-E spike (red) and Delta ΔRBD-E spike with wild-type NTD (green). Negative values for % neutralization indicate enhanced infectivity (**a, b**). The data from quadruplicates are presented as mean ± SEM. The representative data from three independent experiments are shown.

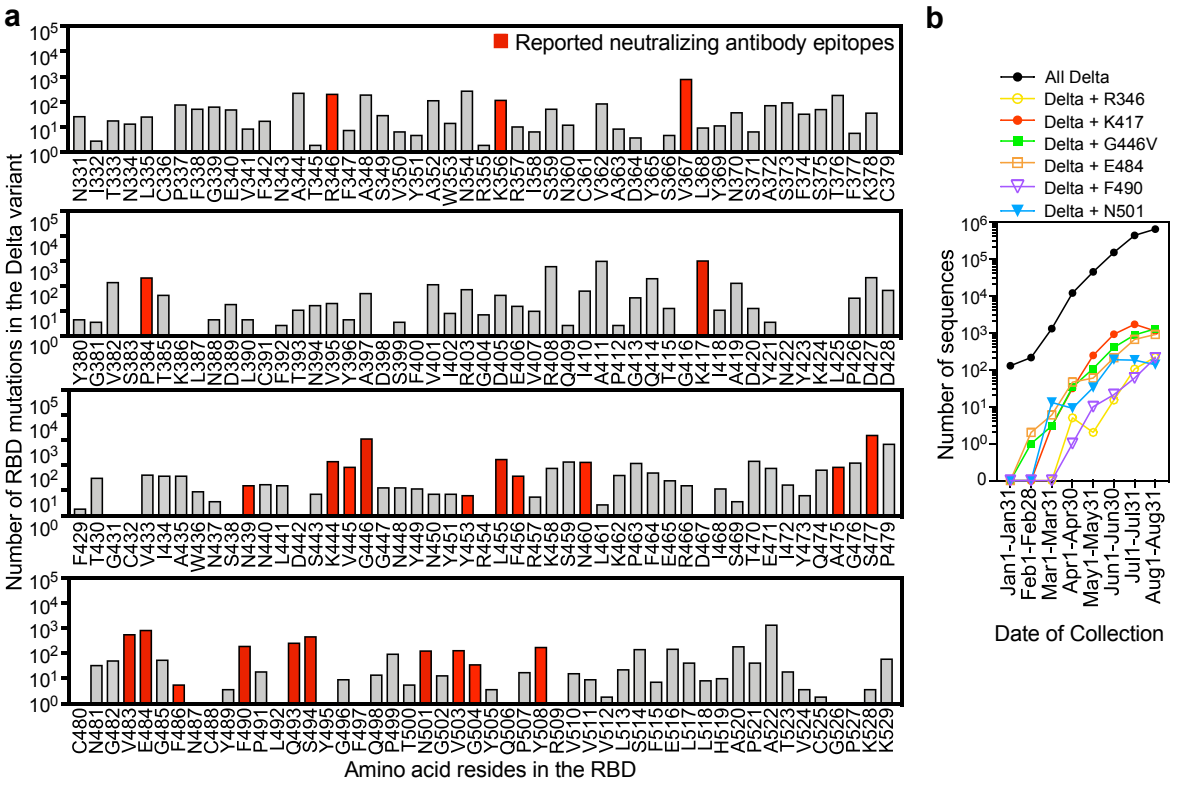

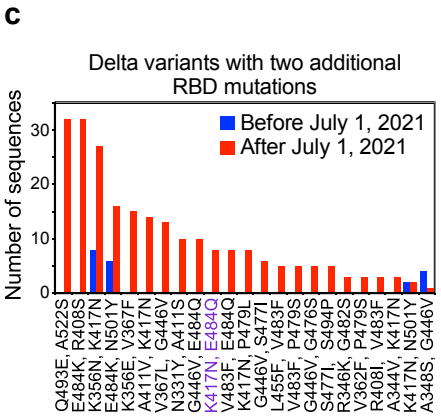

d

The Delta variants with multiple mutations at the RBD

Additional mutations	Accession No. Detected country	Mutations at at RBD
0	Delta	L452R T478K
2	EPI_ISL_4773223 UK	L452R T478K K417N E484Q
2	EPI_ISL_4533975 India	L452R T478K K417N E484Q
2	EPI_ISL_4533957 India	L452R T478K K417N E484Q
2	EPI_ISL_4533956 India	L452R T478K K417N E484Q
2	EPI_ISL_4533950 India	L452R T478K K417N E484Q
2	EPI_ISL_4533943 India	L452R T478K K417N E484Q
2	EPI_ISL_4533921 India	L452R T478K K417N E484Q
2	EPI_ISL_4518977 USA	L452R T478K K417N E484Q
3	EPI_ISL_4521308 Sweden	L452R T478K G446V Y453F G476S
3	EPI_ISL_4324248 France	L452R T478K G446V Y453F S477I
3	EPI_ISL_4293812 France	L452R T478K L455F V483F E484K
3	EPI_ISL_3502562 Spain	L452R T478K N501Y E484K F497S
4	EPI_ISL_4521392 Sweden	L452R T478K G446V Y453F G476S S494P
5	EPI_ISL_4280668 France	L452R T478K P337S L455F V483F E484K N501Y
4	Delta ΔRBD-E	L452R T478K K417N N439K E484K N501Y

Extended Data Fig. 4. RBD mutations acquired by the Delta variants

a, Number of RBD mutations acquired by the Delta variant. The numbers of mutations at each residue registered in the GISAID database are shown. Samples collected from August 1st to August 31th were analysed. L452 and T478 mutations included in all the Delta variant were excluded. The red bars indicate the known epitopes for anti-RBD neutralizing antibodies. **b,** Number of the Delta variants with additional mutations at the RBD. **c,** Number of the Delta variants with two additional mutations at the RBD in the samples collected before July 1st (blue) or after July 1st (red). The Delta variant with K417N and E484Q mutations (Delta 2+) was indicated (purple). **d,** GISAID accession number of the Delta variants with multiple mutations at RBD were shown. L452R and T478K mutations are observed in all the Delta variants (purple). Delta variants with deletions of F157 and R158 at the NTD, characteristic of the representative Delta variant, were selected in **(c)** and **(d)**.

a

The Mu variants with multiple mutations at the RBD

Additional mutations	Accession No.	Mutations at RBD
0	Mu	R346K E484K N501Y
1	Mu + K417N (~10% of Mu)	R346K E484K N501Y K417N
2	EPI_ISL_3695766 EPI_ISL_4360532	R346K E484K N501Y K417N K444R
2	EPI_ISL_4201406 EPI_ISL_4463993	R346K E484K N501Y K417N Q498R
2	EPI_ISL_3274589 EPI_ISL_3769085	R346K E484K N501Y K417N L452R

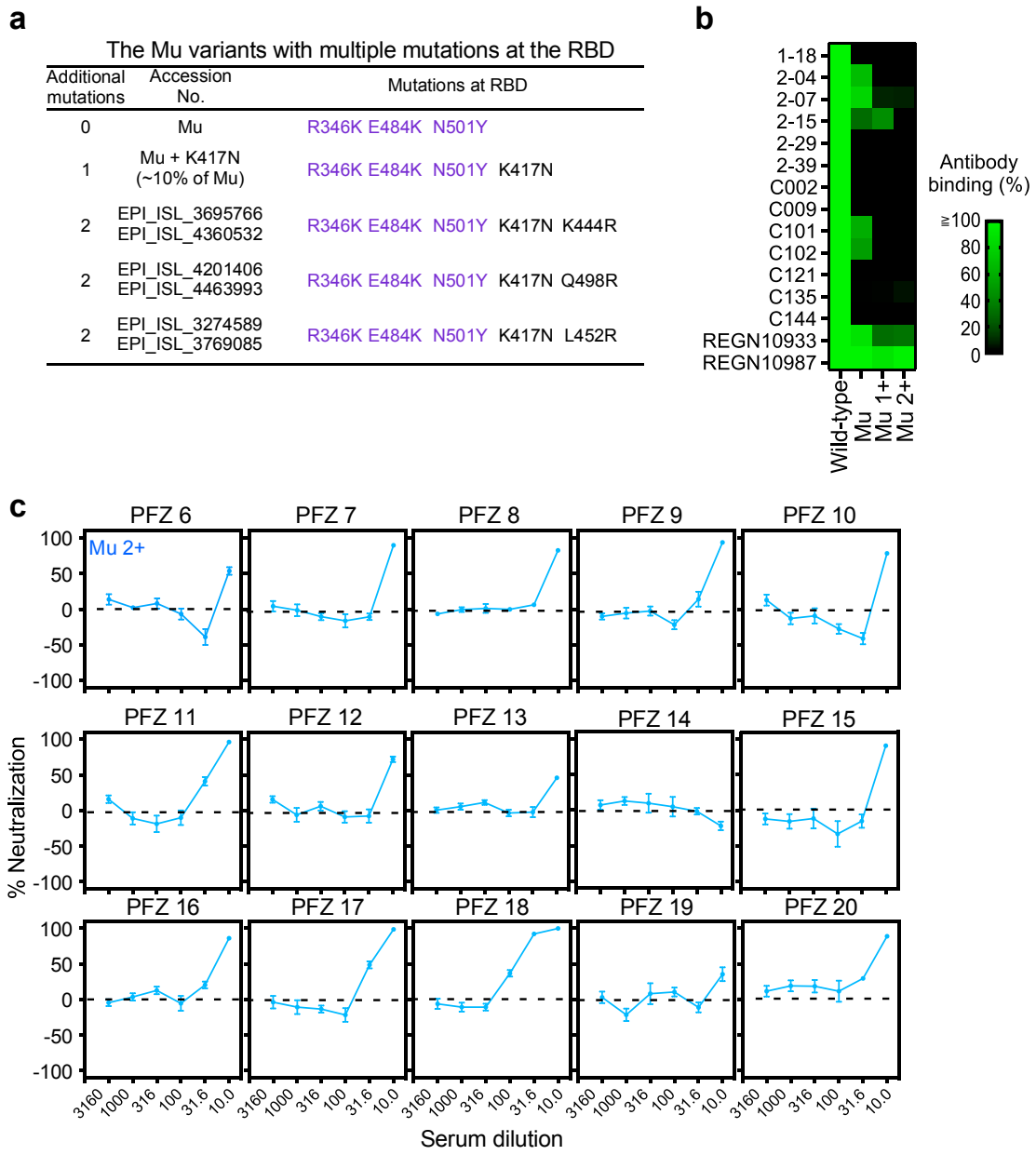

Extended Data Fig. 5. Acquisition of resistance to wild-type spike-immune sera by SARS-CoV-2 Mu variant.

a, GISAID accession number of the Mu variants with additional mutations at RBD were shown. R346K, E484K and N501Y mutations are observed in all the Mu variants (purple). Representative Mu variants with asparagine insertion at the residue 145 of the NTD were selected. **b,** Anti-RBD antibody binding to the Mu spike with additional mutations at the RBD compared with the wild-type spike. Mu 1+: R346K, E484K, N501Y, K417N; Mu 2+: R346K, E484K, N 501Y, K417N, L452R. **c,** Neutralizing activity of the 15 out of twenty BNT162b2-immune sera, not shown in **Fig. 3h**, against the pseudovirus with Mu spike with two additional mutations (Mu 2+: K417N and L452R). Negative values for % neutralization indicate enhanced infectivity. The data from quadruplicates are presented as mean ± SEM. The representative data from three independent experiments are shown.

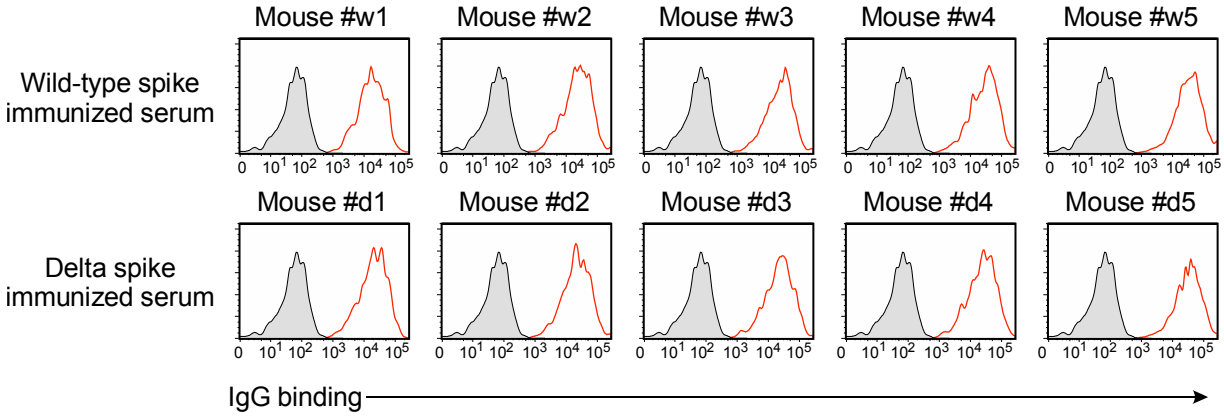

Extended Data Fig. 6. Anti-spike antibodies of the wild-type and delta spike-immunized mice.

IgG antibody binding of the 100 times diluted spike-immunized mouse sera to the wild-type spike transfectants were analysed by flow cytometer. Red: IgG binding. Gray: Control staining.

Extended Data Table 1. Cryo-EM data collection and processing statistics

Data collection		
Sample		Spike protein of SARS-CoV2 Delta strain
Micorscope		Titan Krios
Acc. Voltage (kV)		300
Total electron dose (e^-/A)		50
Pixel size (A)		0.88
Defocus range (μm)		-0.8 – -2.0 (0.15)
Magnification		81,000
Corrected Cs (mm)		0.064
Data processing		
Software		CryoSparc v3.2.0
# of Micrographs		15,000
# of particles		147,497
Symmetry		C1
Resolution (Å, GS-FSC=0.143)		3.19
EMDB ID		31731
Model building		
Method		Rigid body fitting & Coot
Template model		AlphaFold2 prediction, 7JJI, 7N01
# of Atoms		21,634 (2,725 residues)
modification		NAG: 27
MolProbity score		2.07
Map vs model resolution (FSC = 0.5)		3.3 (masked)
Ramachandran (%)	Favored	90.54
	Allowed	9.16
	Outlier	0.30
Clash score		10.42
CaBLAM outeliers (%)		4.15
RMSZ bound length (A)		0.006
RMSZ bound angle (°)		0.814
PDBID		7V5W